ASTRO-H

INSTRUMENT CALIBRATION REPORT
SXI CONTAMINATION
ASTH-SXI-CALDB-CONTAMI

Version 1.1

22 December 2016

ISAS/ GSFC

Prepared by: Eric D. Miller, M. Nobukawa, H. Nakajima

Table of Contents

1 Introduction 4
1.1 Purpose 4
1.2 Scientific Impact 4
2 Release CALDB 20160310 4
2.1 Data Description 4
2.2 Data Analysis 5
2.3 Results 9
2.4 Comparison with Previous Results 9
2.5 Final Remarks 9

CHANGE RECORD PAGE (1 of 1)

DOCUMENT TITLE : SXI Contamination			
ISSUE	DATE	PAGES AFFECTED	DESCRIPTION
Version 1.0	March 2016	All	First Release
Version 1.1	22 Dec 2016	Section 2	Updated with analysis of in-flight data, and more detail about the CALDB file contents. There is no change in the CALDB file.

1 Introduction

1.1 Purpose

This document describes how the contamination CALDB file for the Soft X-ray Imager (SXI) is prepared. The CALDB file structure is define in the ASTH-SCT-04 and available from the CALDB web page at http://hitomi.gsfc.nasa.gov.

1.2 Scientific Impact

The contamination CALDB file contains information about any build-up of molecular contamination in the optical path of the SXI. Such contamination reduces the soft X-ray response of the instrument (below ~ 1 keV), and introduces absorption edges that depend on the chemical composition. The contamination can be spatially variable, so the effect must be measured in a number of subregions across the SXI field of view. At the start of the mission, the contamination is assumed to be zero.

2 Release CALDB 20160310

Filename	Valid date	Release date	CALDB Vrs	Comments
ah_sxi_contami_20140101v001.fits	2014-01-01	20160310	001	

2.1 Data Description

Extension	**Content**
PRIMARY	Blank
COLUMN_DENSITY	Column density and covering fraction of 3 contamination components vs. time and subregion
COLUMN_TRANS	Transmission of 3 components vs. energy
SUBREGION	CCD, segment and ACT and DET coordinates of the four corners of each subregion

The CALDB file contains three binary table extensions, summarized in the table above. The first extension contains the column density and covering factor as a function of time and subregion for three different chemical components. Since the contamination is assumed to be zero at the beginning of the mission, a single time stamp is used, and for each chemical component the column density is populated with zeros and the covering factor is populated with ones.

The second extension contains the transmission curves for a column density of $1x10^{18}$ cm^{-2} of each component. In the current version, these components are assumed to be hydrogen; carbon (with a C K absorption edge at 0.28 keV); and oxygen (with an O K absorption edge at 0.53 keV). The transmission curves were generated from the XSPEC *varabs* model, assuming Verner

et. al. (1996) photoelectric absorption cross-sections, and are reported in 5 eV bins. The curves are shown in Figure 1.

The third extension contains information about the subregion locations, providing the CCD_ID and SEGMENT, and the four corners of each subregion in ACT and DET coordinates. Each is a 20x20 pixel square, so each of the four SXI CCDs contains 32x32 (1024 total) subregions, for a total of 4096 subregions over the SXI field of view.

2.2 Data Analysis

In-orbit measurement of the contamination has been performed with multiple observations of RXJ1856-3754 with an interval of one week. The following datasets from v2 of the data release were used:

Sequence and DATACLASS	DATE_OBS	DATE_END
ah100043030sxi_p0100004f0	2016-03-18T16:27	2016-03-19T13:18:03
ah100043040sxi_p0100004f0	2016-03-19T14:44	2016-03-19T16:30:07
ah100043050sxi_p010000530	2016-03-23T14:47	2016-03-24T10:53:54
ah100043060sxi_p010000530	2016-03-24T11:35	2016-03-25T10:13:21

Only non-MZDYE data were used for the analysis to avoid effects of light-leak. The data were reprocessed with *sxipipeline* using "Hitomi_19Dec2016_V004_pre5" (essentially the Version 5 software) and the following CALDB files:

```
ah_sxi_chtrail_20140101v002.fits
ah_sxi_cti_20140101v002.fits
ah_sxi_gain_20140101v002.fits
ah_sxi_pattern_20140101v001.fits
ah_sxi_spth_20140101v001.fits
ah_sxi_vtevnodd_20140101v002.fits
```

Spectra were extracted from a 2.5 arcmin radius circle centered on the source, using a background region elsewhere on the same aimpoint segment. The RMF, exposure map, and ARF were constructed using:

```
ah_sxi_rmfparam_20140101v002.fits
ah_sxi_instmap_20140101v003.fits
ah_sxi_quanteff_20140101v001.fits
ah_sxi_contami_20140101v001.fits
ah_sxi_telarea_20140101v002.fits
```

In particular, a bug in *aharfgen* pre-Version 5 was corrected in these ARFs. When `CONTAMIFILE=CALDB` or `<filename>` was specified, a small amount of contamination was introduced even if CALDB values are zero (the subregion weighting values were not properly initialized). Specifying `CONTAMIFILE=NONE` produces a zero contamination ARF. This bug is fixed in Version 5, and `CONTAMIFILE=NONE` was used here to ensure zero contamination in the ARF. The differences between the two ARFs are shown in Figure 2.

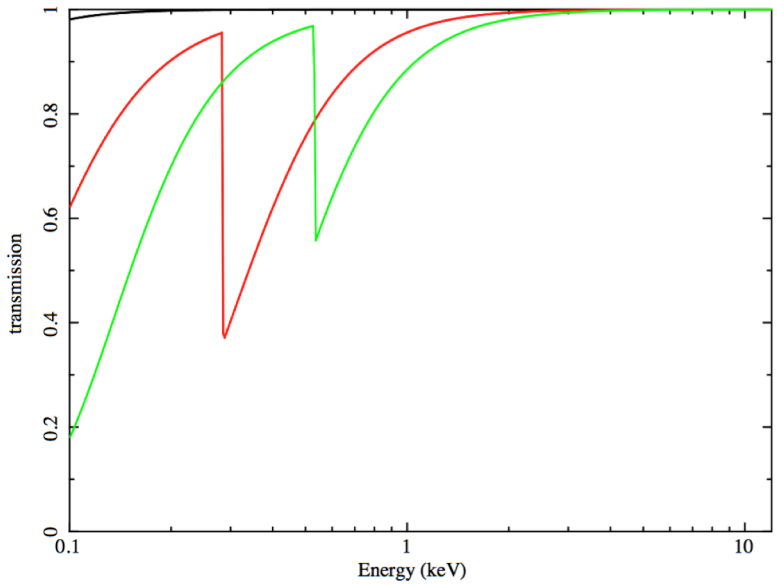

Figure 1. Transmission curves in the SXI contamination CALDB file. These are tabulated for a column density of $1x10^{18}$ cm^{-2} of hydrogen (black), carbon (red), and oxygen (green).

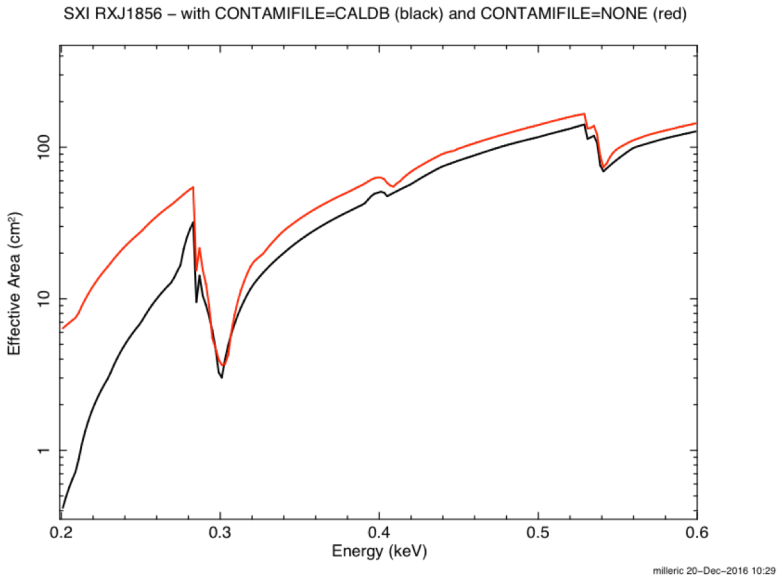

Figure 2. Effective area curves for the *aharfgen* bug which produces a small amount of contamination. Black is incorrect, red is correct.

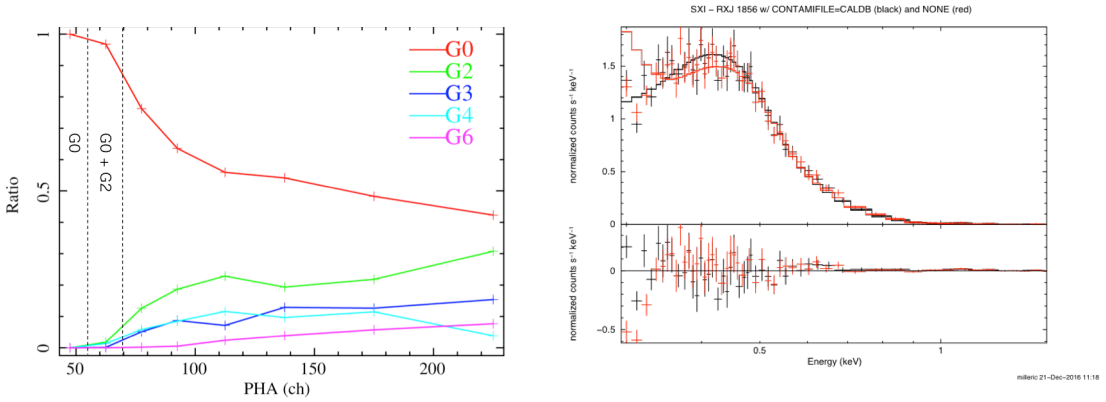

Figure 3. (Left) Grade-branching ratios from RXJ1856 data showing the fraction of single-pixel (G0) and split-pixel (G2346) events. Below PHA = 90 ADU (~0.54 keV), many split events are lost below the event and split thresholds. (Right) Spectral fits using the incorrect (black) and correct (red) ARF, to show that count rate below 0.4 keV is likely reduced because of the event and split thresholds.

The spectral model used comes from Beuermann et al. (2006, A&A, 458,541) from analysis of *Chandra* LETG, *ROSAT,* and *EUVE* data. It consists of two blackbodies with temperatures of 63 and 32 eV, absorbed by Galactic N_H. An additional *hcnocol* absorption component was used to model the contamination, specifying column densities of H, C, N, and O in units of 10^{18} cm^{-2}, and assuming Verner cross-sections. Only the C column density was allowed to vary freely for each observation. The normalizations were not allowed to vary, including an overall constant factor fixed at unity.

Since the event threshold was set to 40 ADU (~ 0.24 keV) for these observations, some split events might be lost below the event threshold. From *Chandra* and *Suzaku* experience, this effect occurs at energies $E < EventTH + n \times SplitTH$, for n = 3–4. For a split threshold of 15 ADU, this cut-off is 0.5-0.6 keV. This is consistent with the grade branching ratios in Figure 3, which show that below PHA = 90 ADU (~0.54 keV), the detected X-rays are dominated by single-pixel events. Also shown in Figure 3 are spectral fits using the incorrect (black) and correct (red) ARF. The region below 0.4 keV fits well with the incorrect ARF, however the count rate is well below the model using the correct ARF. This is likely due to the event and split threshold. As a result, only data above 0.5 keV are used in the final fit, although fits down to 0.3 keV are consistent.

The best-fit parameters are shown below for various energy ranges and for the incorrect and correct ARF. The fits assume wilm abundances, verner cross-sections, and use C-stat as the fit statistics with no spectral grouping. The spectra have been binned only in the plots. The non-varying parameters are only shown in the first table for reference.

Fit with incorrect ARF (black) and correct ARF (red) to `ah100043060sxi_p010000530` 0.3–1.5 keV. Spectra are in Figure 3.

```
#========================================================================
#Model TBabs<1>(bbodyrad<2> + bbodyrad<3>)constant<4>*hcnocol<5> Source No.: 1   Active/On
#Model Model Component  Parameter  Unit     Value
# par  comp
#                            Data group: 1
#   1    1   TBabs      nH         10^22    1.10000E-02  frozen
#   2    2   bbodyrad   kT         keV      6.28300E-02  frozen
#   3    2   bbodyrad   norm               1.42884E+05  frozen
#   4    3   bbodyrad   kT         keV      3.22600E-02  frozen
#   5    3   bbodyrad   norm               1.87964E+06  frozen
#   6    4   constant   factor             1.00000      frozen
#   7    5   hcnocol    H          sC18     0.0          frozen
#   8    5   hcnocol    C          sC18     -3.88711E-02 +/-  3.46307E-02
#   9    5   hcnocol    N          sC18     0.0          frozen
#  10    5   hcnocol    O          sC18     0.0          frozen
#                            Data group: 2
#  11    1   TBabs      nH         10^22    1.10000E-02  = p1
#  12    2   bbodyrad   kT         keV      6.28300E-02  = p2
#  13    2   bbodyrad   norm               1.42884E+05  = p3
#  14    3   bbodyrad   kT         keV      3.22600E-02  = p4
#  15    3   bbodyrad   norm               1.87964E+06  = p5
#  16    4   constant   factor             1.00000      = p6
#  17    5   hcnocol    H          sC18     0.0          = p7
#  18    5   hcnocol    C          sC18     0.621581     +/-  3.74639E-02
#  19    5   hcnocol    N          sC18     0.0          = p9
#  20    5   hcnocol    O          sC18     0.0          = p10
#________________________________________________________________________
#Fit statistic : C-Statistic =        542.755 using 402 PHA bins and 400 degrees of freedom.
#Test statistic : Chi-Squared =        596.558 using 402 PHA bins.
# Reduced chi-squared =        1.49139 for    400 degrees of freedom
# Null hypothesis probability =   6.063244e-10
```

Fit with correct ARF, all four sequences, 0.3–1.5 keV. Spectra in Figure 4.

```
#========================================================================
ah100043030sxi_p0100004f0     2016-03-18T16:27
#   8    5   hcnocol    C          sC18     0.717182     +/-  4.68429E-02
ah100043040sxi_p0100004f0     2016-03-19T14:44
#  18    5   hcnocol    C          sC18     0.725804     +/-  0.130032
ah100043050sxi_p010000530     2016-03-23T14:47
#  28    5   hcnocol    C          sC18     0.670801     +/-  4.14738E-02
ah100043060sxi_p010000530     2016-03-24T11:35
#  38    5   hcnocol    C          sC18     0.621581     +/-  3.74639E-02
#________________________________________________________________________
#Fit statistic : C-Statistic =       1082.357 using 804 PHA bins and 800 degrees of freedom.
#Test statistic : Chi-Squared =       1217.949 using 804 PHA bins.
# Reduced chi-squared =       1.522436 for    800 degrees of freedom
# Null hypothesis probability =   6.840001e-20
```

Fit with correct ARF, all four sequences, 0.3–1.5 keV. Spectra in Figure 4.

```
#========================================================================
ah100043030sxi_p0100004f0     2016-03-18T16:27
#   8    5   hcnocol    C          sC18     0.726076     +/-  0.143982
ah100043040sxi_p0100004f0     2016-03-19T14:44
#  18    5   hcnocol    C          sC18     0.710763     +/-  0.398205
ah100043050sxi_p010000530     2016-03-23T14:47
#  28    5   hcnocol    C          sC18     0.613143     +/-  0.126530
ah100043060sxi_p010000530     2016-03-24T11:35
#  38    5   hcnocol    C          sC18     0.482538     +/-  0.113370
#________________________________________________________________________
#Fit statistic : C-Statistic =        716.516 using 668 PHA bins and 664 degrees of freedom.
#Test statistic : Chi-Squared =        748.774 using 668 PHA bins.
# Reduced chi-squared =        1.12767 for    664 degrees of freedom
# Null hypothesis probability =   1.215569e-02
```

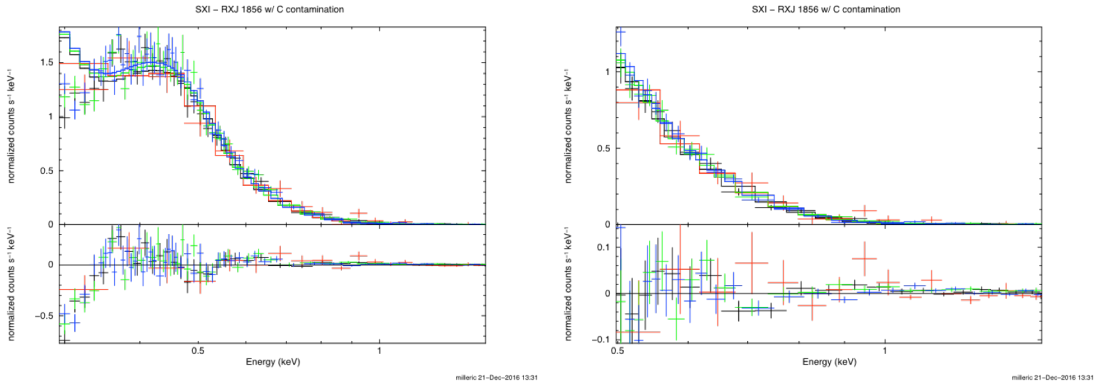

Figure 4. Spectral fits for the four sequences in the energy ranges 0.3–1.5 (left) and 0.5–1.5 (right).

2.3 Results

The spectral fits are consistent with carbon contamination of $N_C = (6 \pm 1) \times 10^{17}$ cm^{-2}. There is also some evidence of a negative oxygen edge, which remains unsolved. The measured contamination shows no statistically significant time evolution over the one week time. Due to lack of additional data at low energies and at other epochs and locations on the focal plane, it is impossible to conclude that molecular contamination is indeed responsible for the reduction in effective area at soft energies.

The transmittance produced by this contamination is shown in Figure 5. Above 1.5 keV, there is less than a 1% reduction in count rate. At 1 keV it is 3%, at 0.8 keV it is 5%. Since all *Hitomi* observations except RXJ1856 were obtained with event threshold of 100 ADU (~0.6 keV), the reliable lower limit of spectral analysis due to loss of split events is ~ 0.9 keV. Therefore this level of contamination has no effect on data aside from RXJ1856, and zero contamination can be assumed. The CALDB file has not been updated from pre-flight values. For analysis of RXJ1856 on the other hand, it is important to include this contamination component.

2.4 Comparison with Previous Results

These are the first in-flight data, so there are no previous results to compare. The results are inconsistent with zero contamination, which was assumed at the launch of *Hitomi*.

2.5 Final Remarks

This is the final release of this CALDB file.

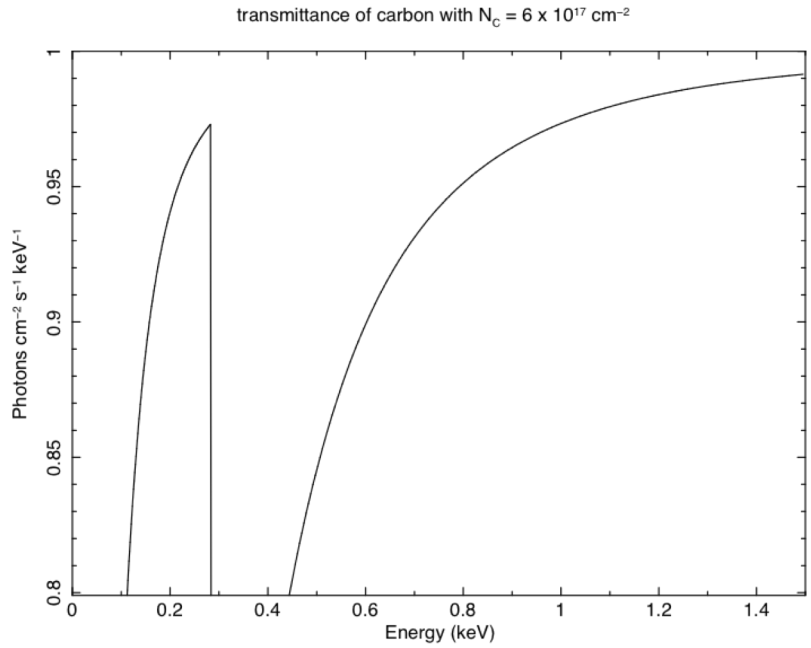

Figure 5. Transmittance of the measured contamination as a function of energy. Note the Y axis label is incorrect.